

ANALYSIS OF THE IMPACT OF ASH AND SCALE FOULING ON THE SUPERHEATER OPERATION

M. Trojan¹, D. Taler², and J. Taler¹

¹ Institute of Thermal Power Engineering, Cracow University of Technology, Al. Jana Pawla II 37, 31-864 Cracow, Poland
 E-mail (Corresponding author): taler@mech.pk.edu.pl

² Institute of Thermal Engineering and Air Protection, Cracow University of Technology, Cracow, Poland

ABSTRACT

Numerical modeling of steam superheaters presented in the paper can be used for detailed analysis of flow and thermal phenomena in superheaters. Mathematical simulation of superheater operation considering fouling processes on the flue gas and steam side is a useful tool to extend the lifetime of superheater tubes. Superheater model was used to analyzing the impact of ash deposits on the outer tube surfaces and scales formed on the inner tube surfaces on the heat flow rate transferred from the flue gas to the steam. Ash fouling causes a significant decrease in heat flux absorbed by the superheater. In addition, ash fouling lowers the temperature of the steam and the tube wall. Scaling on the inner surface of the tube results also in the reduction of heat flux transferred from the flue gas to the steam. In contrast to the ash fouling, it also causes a significant increase in wall temperature of superheater tubes, despite a decrease in the absorbed heat. As in the case of ash fouling, scale deposits on the inner surface of the tube contributes to lowering the steam temperature at the outlet of the superheater.

INTRODUCTION

Superheaters are tubular cross-flow heat exchangers. However, they differ very significantly from the other heat exchangers operating at moderate temperatures. The characteristic feature of the superheaters is complicated flow arrangement and high water steam and flue gas temperature. Because of the high dependence of the water steam specific heat on pressure and temperature, the superheater cannot be calculated as a typical heat exchanger using conventional methods (Hewitt et al., 1994) such as the ϵ -NTU method (effectiveness – number of transfer units) or the method based on the logarithmic mean temperature difference between the fluids (the LMTD method). Mathematical modeling of superheaters is the subject of few publications despite the great practical significance of the problem. The main reason for this situation is the difficulty of the description of complex flow and thermal phenomena in the steam superheaters both in pulverized coal and fluidized boilers.

Many difficulties in the operation of coal-fired steam boilers make slagging and fouling of water-walls and superheaters. Experimental and CFD simulations of fireside slagging and fouling are presented in the works (Wieland et al., 2012; Weber et al., 2013; Leppänen et al., 2014). The emphasis was placed on examining various approaches used to predict the slag deposition (Wieland et al., 2012; Weber et al., 2013) and on numerical modeling of fine particle and deposit formation in a recovery boiler (Leppänen et al., 2014). However, the impact of slag and ash deposits on the tube wall temperature and the temperature of the steam was not analyzed.

In this paper, a numerical model of the entire boiler including superheater stages has been developed. The model allows determining the degree of slag and ash deposition on the water-walls and superheaters, respectively.

Based on measurements carried out on the side of flue gas and steam, the thermal efficiency of the water-walls, which is a measure of water-wall slagging, and the thermal resistance of ash deposits on the individual stages of the superheater were determined.

SLAGGING OF FURNACE WATERWALLS AND FOULING OF SUPERHEATERS

Deposits are formed on the furnace water-walls and superheater surfaces if the ash in the flue gas is at a temperature above its melting point. A deposit is usually formed if the flue gas temperature is over 1200°C. The heat flow rates, \dot{Q}_{ev} and \dot{Q}_{sup} , are determined using the measured data from the following expressions (Fig. 1)

$$\dot{Q}_{ev} = (\dot{m}_s - \dot{m}_{w1} - \dot{m}_{w2}) h''(p_d) + \dot{m}_b h'(p_d) - \dot{m}_{fw} h_{fwh} \quad (1)$$

$$\dot{Q}_{sup} = (\dot{m}_s - \dot{m}_{w1} - \dot{m}_{w2}) [h_1 - h'(p_d)] + (\dot{m}_s - \dot{m}_{w2})(h_3 - h_2) + \dot{m}_s (h_s - h_4) \quad (2)$$

The temperature T'_{fe} of the flue gas exiting the furnace, expressed in K, is given by

$$T'_{fe} = T_{gs} + \frac{\dot{Q}_{sup}}{\dot{m}_g \cdot c_{p,g} \Big|_{T_{gs}}^{T'_{fe}}} + 273.15 \quad (3)$$

The mass flow rate of live steam is given by

$$\dot{m}_s = \frac{\dot{Q}_{ev}}{h''(p_d) - h_{fwh}} - \dot{m}_b \frac{h'(p_d) - h_{fwh}}{h''(p_d) - h_{fwh}} + \dot{m}_{w1} + \dot{m}_{w2} \quad (4)$$

where \dot{Q}_{ev} denotes the rate of heat transferred by radiation and convection from the combustion chamber to the surrounding waterwalls. Heat transfer rate \dot{Q}_{ev} can be calculated from the expression

$$\dot{Q}_{ev} = \dot{Q} - \dot{m}_g \cdot c_{p,g} \Big|_0^{T_{fe}} \cdot T_{fe} \quad (5)$$

where \dot{Q} is the heat transfer rate entering combustion chamber with coal and air given by

$$\dot{Q} = \dot{m}_g \cdot c_{p,g} \Big|_0^{T_{ad}} \cdot T_{ad} \quad (6)$$

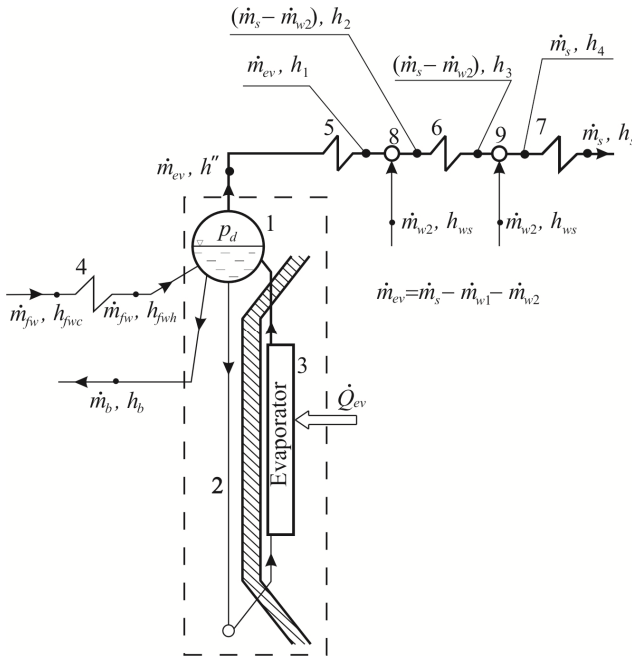


Fig. 1 Control volume for mass and energy balance of boiler evaporator: 1– drum, 2 – downcomers, 3 – evaporator, 4 – economizer, 5 – 1st stage superheater, 6 – platen superheater, 7 – 2rd and 3rd stage superheater, 8 – 1st stage superheater attemperator, 9 – 2nd stage superheater attemperator.

The adiabatic temperature of combustion t_{ad} expressed in °C is given by

$$t_{ad} = \frac{\dot{m}_F (H_{LV} + h_F) + \dot{m}_a \cdot c_{p,a} \Big|_0^{t_a}}{\dot{m}_g \cdot c_{p,g} \Big|_0^{t_{ad}}} \quad (7)$$

Based on extensive experimental results, relation presented below was found for the calculation of the outlet flue gas temperature T_{fe}/T_{ad} (Blokh, 1988; Kuznetsov et al., 1973)

$$\frac{T_{fe}}{T_{ad}} = \frac{1}{M \left(\frac{\varepsilon_f}{Bo} \right)^{0.6} + 1} \quad (8)$$

where M is a parameter accounting for the kind of fuel (coal, oil or gas) and burners location. Both temperatures T_{fe} and T_{ad} appearing in Eq. (8) are expressed in Kelvin.

The Boltzmann number Bo is defined as

$$Bo = \frac{\dot{m}_g \cdot \bar{c}_{p,g}}{\sigma \cdot \psi \cdot A_w \cdot T_{ad}^3} \quad (9)$$

The mean specific heat $\bar{c}_{p,g}$ over the temperature range $[t_{fe}, t_{ad}]$ is

$$\bar{c}_{p,g} = \frac{c_{p,g} \Big|_0^{t_{ad}} \cdot t_{ad} - c_{p,g} \Big|_0^{t_{fe}} \cdot t_{fe}}{t_{ad} - t_{fe}} \quad (10)$$

The emissivity of the combustion chamber ε_f is given by

$$\varepsilon_f = \frac{\varepsilon_{fl}}{\varepsilon_{fl} + (1 - \varepsilon_{fl}) \psi} \quad (11)$$

where ε_{fl} is the flame emissivity, and ψ is the effectiveness of the combustion chamber waterwalls defined as the ratio of the absorbed to the incident heat flux.

The waterwall effectiveness ψ is estimated in the on-line mode from the following nonlinear equation

$$\dot{m}_s^m = \dot{m}_s^c(\psi) \quad (12)$$

where \dot{m}_s^m and \dot{m}_s^c is measured and calculated steam mass flow rate, respectively. The mass flow rate \dot{m}_s^c is calculated using Eq.(4) as a function of the waterwall effectiveness ψ . The symbol \dot{m}_s^m stands for measured flow rate with the orifice plate at the outlet of the boiler.

MATHEMATICAL MODEL OF THE SUPERHEATER

Ash deposits on externals surfaces reduce slight tube wall temperatures. The impact of steam- side scale deposits is reversed. Due to the low thermal conductivity, the temperature increase over the scale layer is high. This leads to a higher tube wall temperature that in turn reduces the superheater lifetime considerably. To simplify the analysis,

the steam-side oxide scale is considered to be a single-layered oxide deposit of uniform thickness δ_s .

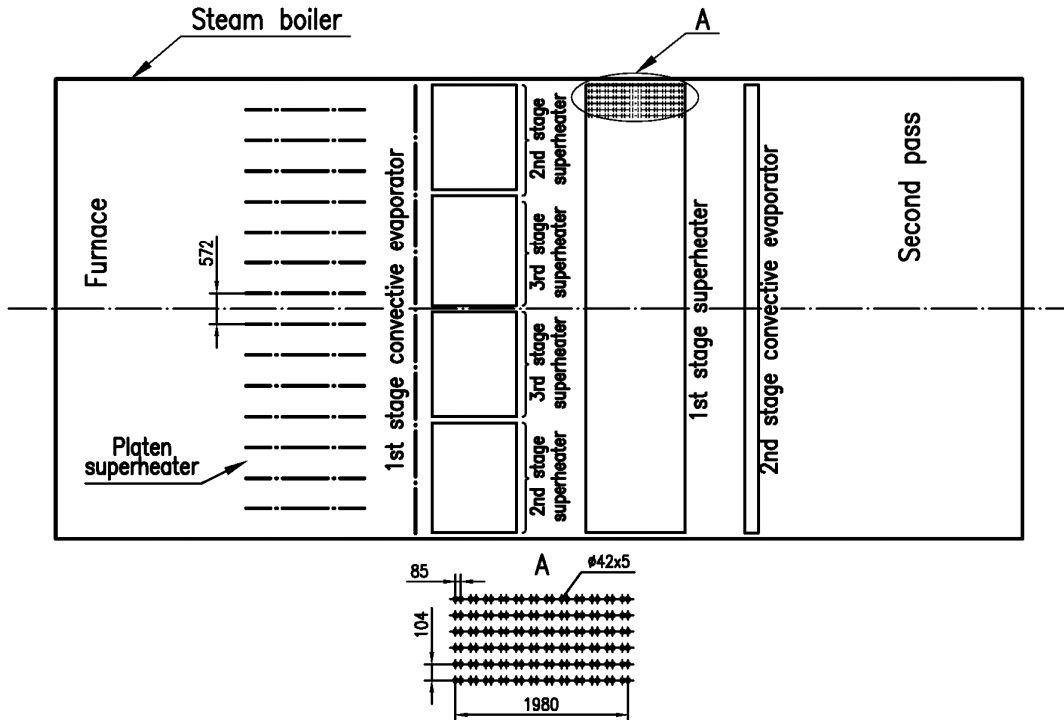


Fig. 2 Arrangement of boiler heating surfaces.

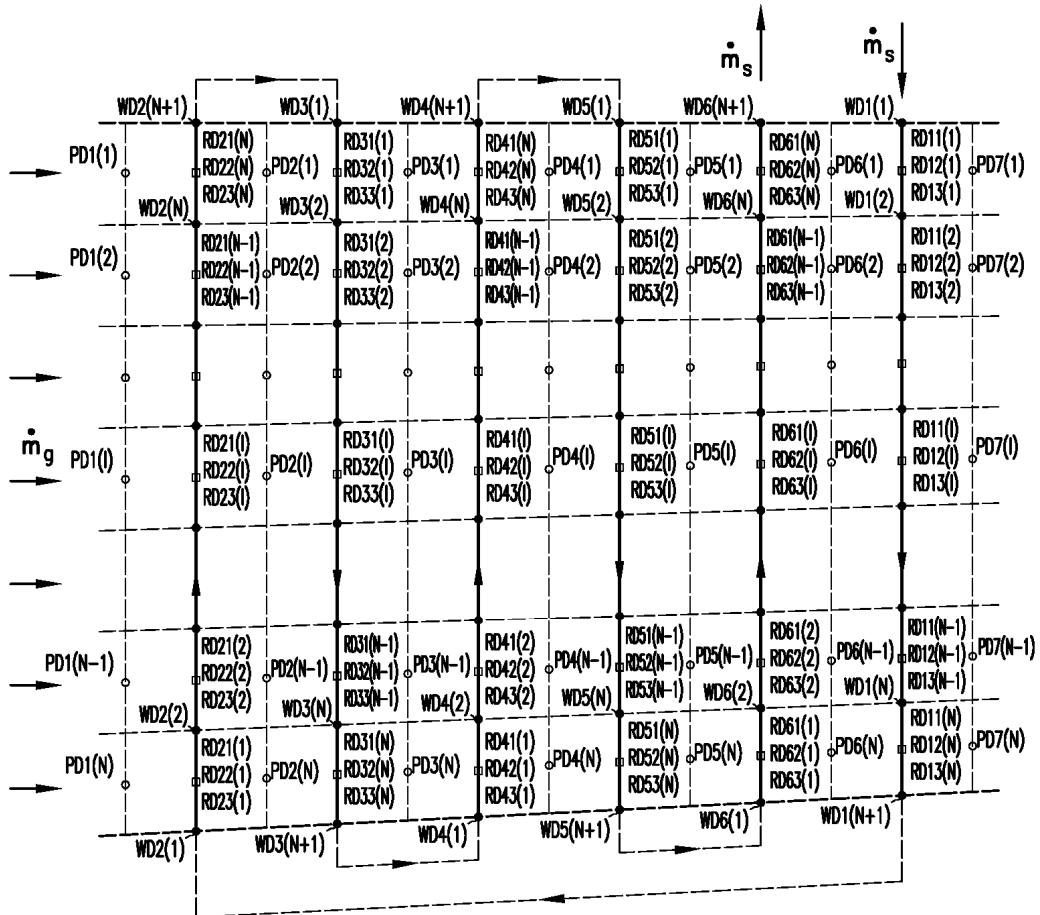


Fig. 3 Second stage superheater flow arrangement and division of superheater into control volumes; o - flue gas, • - water steam, □ - tube wall; PD1(1),...,PD1(N) – flue gas temperature at the nodes before the superheater, WD1(1),...,WD1(N+1) – steam temperature at the nodes in the first superheater pass.

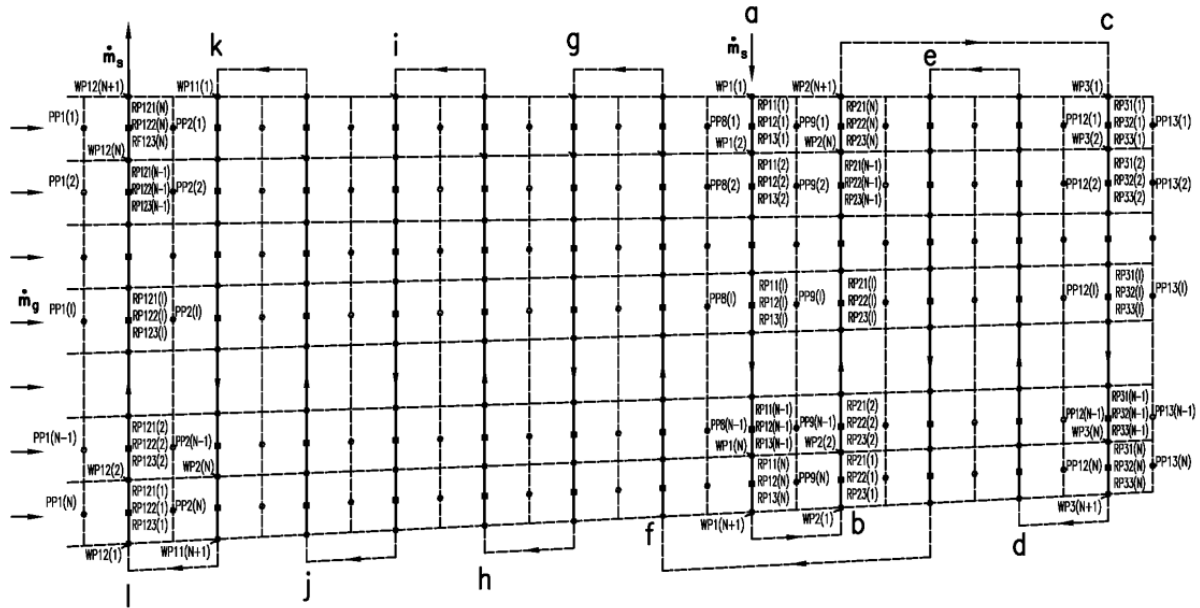


Fig. 4. First stage superheater flow arrangement and division of superheater into control volumes; o - flue gas, • - water steam, □ - tube wall; PP1(1),...,PP1(N) – flue gas temperature at the nodes before the superheater, WP1(1),...,WP1(N+1) – steam temperature at the nodes in the first superheater pass.

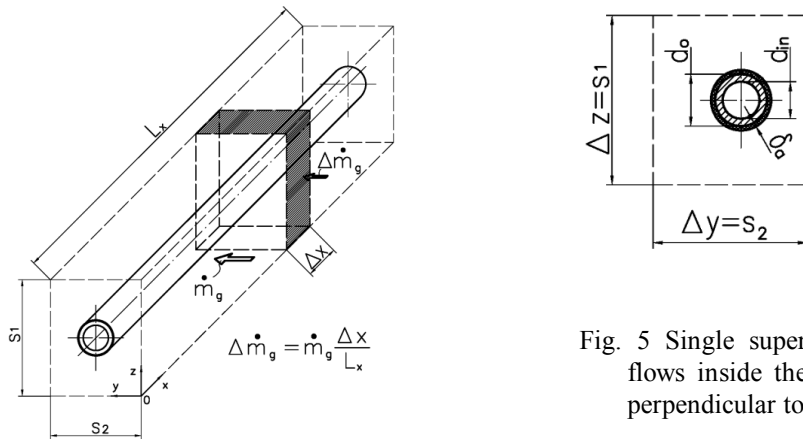


Fig. 5 Single superheater tube; water steam flows inside the tube, and flue gas flows perpendicular to the tube axis.

The presence of iron oxides with the thermal conductivity k_s on the inner surfaces of superheater tubes will be taken into account by introducing an equivalent heat transfer coefficient h_e defined as

$$\frac{1}{h_e} = \frac{r_{in}}{k_s} \ln \frac{r_{in}}{r_{in} - \delta_s} + \frac{r_{in}}{r_{in} - \delta_s} \frac{1}{h_s} \quad (13)$$

When the tube inner surfaces are fouled with scales, then in place of the heat transfer coefficient h_s for clean surfaces we have to insert the equivalent heat transfer coefficient h_e .

The location of the superheater in the boiler is shown in Fig. 2. Mathematical models of all superheater stages were built. The finite volume method (FVM) was used to

solve the system of differential equations for temperature of the both fluids and the tube wall with appropriate boundary conditions. Numerical models of multi-pass steam superheater stages with several tube rows (passes) (Figs. 3 and 4) were developed. The convection and radiation heat transfer on the flue gas side was accounted for. The heat transfer coefficient takes into account convection and radiation components. Radiative heat transfer coefficient was calculated according to the method described in (Taler and Taler, 2009).

In addition, the deposits layers will be assumed to cover the inner and outer surfaces of the tubes.

At first a model of the superheater is divided into finite control volumes. As examples of the superheater stages, the

first and the second stage convective superheater will be considered. The flow arrangement and division of these superheater stages into finite volumes are depicted in Figs. 3 and 4. The superheated steam and the combustion products flow at right angles to each other. The first and the second stage convective superheaters can be classified according to flow arrangement as mixed-cross-flow heat exchangers. The superheater tubes are arranged in-line. In the following, finite volume heat balance equations will be formulated for the steam, tube wall, and flue gas.

A basis for the formulating of the mathematical model of the whole superheater is a single tube placed in a cross-flow. The tube arrangement in the superheater is characterized by the longitudinal pitch s_2 parallel to the flue gas flow direction and the pitch s_1 perpendicular to the flue gas flow direction (Fig. 5). The tube cross-flow heat

a) b)

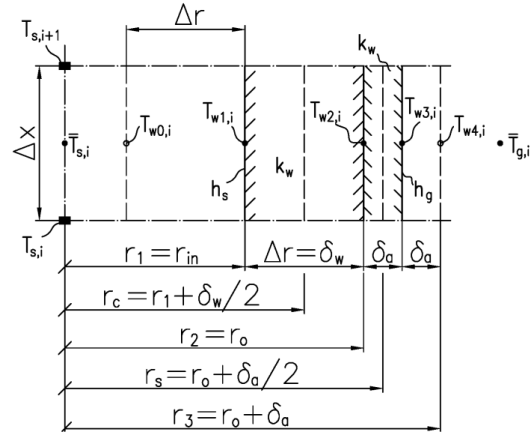
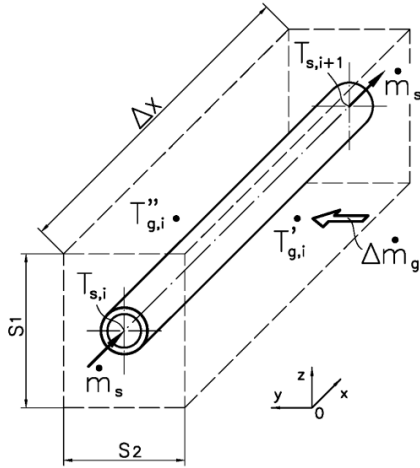


Fig. 6. Finite volumes for the steam and flue gas (a) and for tube wall (b).

After transformation, the energy balance equation (14) can be written as

$$T_{s,i+1} = \frac{1}{1 + \frac{1}{2} \Delta N_{s,i+\frac{1}{2}}} \times \left[\left(1 - \frac{1}{2} \Delta N_{s,i+\frac{1}{2}} \right) T_{s,i} + \Delta N_{s,i+\frac{1}{2}} T_{w1,i} \right], \quad (14)$$

$i = 1, \dots, N$

where the symbol $\Delta N_{s,i+\frac{1}{2}}$ denotes the mesh number of transfer units for the steam.

HEAT BALANCE EQUATIONS FOR TUBE WALL COVERED WITH ASH DEPOSITS

Next, heat balance equations will be formulated for the nodes shown in Fig. 6b. The nodes are located at the inner and outer radius of the tube and outer deposit surface.

exchanger consisting of separate tubes will be replaced by a continuous heat exchanger with a heat transfer surface extending over the entire pitch s_2 (Fig. 5).

HEAT BALANCE EQUATIONS FOR STEAM

A steam side energy balance equation for the i -th finite volume with dimensions $s_1 \times s_2 \times \Delta x$ (Fig. 5 and 6) gives

$$\dot{m}_s c_{ps} \int_0^{T_{s,i}} T_{s,i} + \pi d_{in} \Delta x h_m \left(T_{w1,i} - \frac{T_{s,i} + T_{s,i+1}}{2} \right) = \dot{m}_s c_{ps} \int_0^{T_{s,i+1}} T_{s,i+1} \quad (15)$$

where the symbol $c_{ps} \int_0^{T_s}$ denotes the mean specific heat at constant pressure p in the temperature interval $[0, T_s]$.

Temperature dependent physical properties of the tube material and ash deposits were assumed.

From the heat balance equations for the nodes 1, 2, 3 and 4 we obtain

$$T_{w1,i} = \frac{\left(1 - \frac{\Delta r}{2r_1} \right) T_{w0,i} + \left(1 + \frac{\Delta r}{2r_1} \right) \frac{k_{w2,i} + k_{w1,i}}{k_{w0,i} + k_{w1,i}} T_{w2,i}}{\left(1 - \frac{\Delta r}{2r_1} \right) + \left(1 + \frac{\Delta r}{2r_1} \right) \frac{k_{w2,i} + k_{w1,i}}{k_{w0,i} + k_{w1,i}}}, \quad (16)$$

$i = 1, \dots, N$

$$T_{w2,i} = \frac{\left(1 - \frac{\delta_w}{2r_2} \right) \frac{k_{w1,i} + k_{w2,i}}{2} \frac{T_{w1,i}}{\delta_w} + \left(1 + \frac{\delta_a}{2r_2} \right) \frac{k_{w2,i} + k_{a3,i}}{2} \frac{T_{w3,i}}{\delta_a}}{\left(1 - \frac{\delta_w}{2r_2} \right) \frac{k_{w1,i} + k_{w2,i}}{2} \frac{1}{\delta_w} + \left(1 + \frac{\delta_a}{2r_2} \right) \frac{k_{w2,i} + k_{a3,i}}{2} \frac{1}{\delta_a}}, \quad (17)$$

$i = 1, \dots, N$

$$T_{w3,i} = \frac{\left(1 - \frac{\delta_a}{2r_3}\right) \frac{k_{a2,i} + k_{a3,i}}{2k_{a3,i}} T_{w2,i} + \left(1 + \frac{\delta_a}{2r_3}\right) \frac{k_{a3,i} + k_{a4,i}}{2k_{a3,i}} T_{w4,i}}{\left(1 - \frac{\delta_a}{2r_3}\right) \frac{k_{a2,i} + k_{a3,i}}{2k_{a3,i}} + \left(1 + \frac{\delta_a}{2r_3}\right) \frac{k_{a3,i} + k_{a4,i}}{2k_{a3,i}}},$$

$$i = 1, \dots, N \quad (18)$$

The mean steam temperature $\bar{T}_{s,i}$ and mean gas temperature $\bar{T}_{g,i}$ are defined as follows (Fig. 6)

$$\bar{T}_{s,i} = \frac{T_{s,i} + T_{s,i+1}}{2} \quad \text{and} \quad \bar{T}_{g,i} = \frac{T'_{g,i} + T''_{g,i}}{2}, \quad i = 1, \dots, N \quad (19)$$

Since the change in temperature of the steam and flue gas within a control area is small, the mean arithmetic temperature gives acceptable accuracy.

HEAT BALANCE EQUATIONS FOR FLUE GAS

Heat balance equation for the finite volume shown in Fig. 6 is

$$\Delta \dot{m}_g c_{pg} \Big|_0^{T'_{g,i}} T'_{g,i} = \Delta \dot{m}_g c_{pg} \Big|_0^{T''_{g,i}} T''_{g,i} + \pi (2r_o + 2\delta_a) \Delta x h_g \left(\frac{T'_{g,i} + T''_{g,i}}{2} - T_{w3,i} \right), \quad i = 1, \dots, N \quad (20)$$

After transformation of the heat balance equation (20) and introducing the mesh number of transfer units for the flue gas, Eq. (20) can be written in the form

$$T''_{g,i} = \frac{1}{1 + \frac{1}{2} \Delta N_{g,i+\frac{1}{2}}} \left[\left(1 - \frac{1}{2} \Delta N_{g,i+\frac{1}{2}} \right) T'_{g,i} + \Delta N_{g,i+\frac{1}{2}} T_{w3,i} \right],$$

$$i = 1, \dots, N \quad (21)$$

The non-linear algebraic equations (15), (16)-(18), and (21) were solved by the Gauss-Seidel method.

PRESSURE DISTRIBUTION ON THE STEAM SIDE

The changes of pressure along the steam flow path are determined from the momentum conservation equation for the steady state (Hewitt et al., 1994). The momentum conservation equation for one-dimensional steady flow has the following form

$$\frac{dp}{ds} = -\rho w \frac{dw}{ds} - \rho g \sin \varphi - \frac{\xi}{d_h} \rho \frac{w|w|}{2} \quad (22)$$

where: p - static pressure, Pa; s - coordinate along the flow path in direction of flow; w - steam velocity, m/s; ρ - steam density, kg/m³; φ - angle between tube axis and horizontal plane; ξ - Darcy-Weisbach friction factor; d_h - hydraulic diameter of the superheater tube (for a circular tube, the hydraulic diameter equals the inner diameter of the tube), m.

Using the backward difference quotients to approximate derivatives approximation in Eq. (22) gives

$$p_{i+1} = p_i - \rho_i w_i (w_{i+1} - w_i) - \rho_i g \Delta s \sin \varphi_i - \xi_i \frac{\Delta s}{d_{h,i}} \rho_i \frac{w_i |w_i|}{2} \quad (23)$$

An explicit formula for calculating the friction factor is proposed by Manadilli (Manadilli, 1997). Manadilli developed an explicit formula valid for Re ranging from 5235 to 10^8 and for any value of R_a / d_m

$$\xi = \left[-2 \log \left(\frac{R_a}{3.7 d_m} + \frac{95}{Re^{0.983}} - \frac{96.82}{Re} \right) \right]^{-2} \quad (24)$$

Local resistances are caused by changes in the direction of flow, for example: at entrances, exits, contractions, expansions, elbows and pipe bends, orifices, tees, pipe joints, valves, etc. The formula for the local pressure drop is

$$\Delta p_m = \zeta \frac{w^2}{2} \rho \quad (25)$$

where ζ - the loss coefficient due to local pressure loss.

The loss coefficient for 90° bends with $R/d_m = 4$ is $\zeta = 0.1$. Using the equation (23), it is easy to take into account the local pressure drop assuming that it occurs at the interface between two control volumes. Flue gas pressure drop across the tube bundle can be calculated using experimental correlations given by Gaddis (Gaddis, 2010).

DETERMINING THERMAL RESISTANCE OF ASH DEPOSIT LAYER

The tube outer surface is covered with a layer of ash deposits. Comparing the computed and measured steam

temperature increase over the entire superheater allows for determining the thermal resistance of the deposit layer on the outer surface of the superheater.

The thermal resistance of deposit layer, defined as

$$R = \frac{r_a - r_o}{k_a} \tag{26}$$

was determined from the following nonlinear algebraic equation

$$T_{s,meas} - T_{s,calc} = 0 \tag{27}$$

where $T_{s,meas}$ and $T_{s,calc}$ is the measured and calculated steam temperature at the superheater outlet.

The numerical simulation was carried out for the first stage superheater. The velocity of the flue gas in the smallest cross section between the tubes was equal to 7.69 m / s. The measured temperature of the steam at the outlet of the superheater was 392.7°C and the flue gas temperature behind the superheater was 685.7°C. The thermal resistance of deposit layer was determined from the condition (27), i.e. from the condition of equality of measured and calculated steam temperature at the superheater exit. The determined thermal resistance of the deposits is: $R = 0.00194 / 0.08 = 0.02425 \text{ (m}^2\cdot\text{K)/W}$.

If the superheater is fouled with ash, the outlet steam decreases by about 70K, which results from a reduction in heat flow rate absorbed by the steam. It may be noted that the largest temperature rise occurs in the steam tubes located in the area where the flue gas temperature is high (Fig. 7).

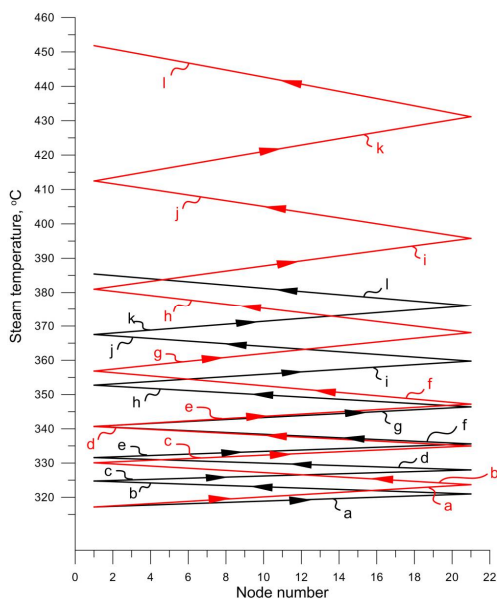


Fig. 7. The temperature distribution along the flow path of water steam for clean first superheater stage (red line) and for superheater fouled by ash deposits (black line).

The steam temperature increase over the length of the tube 1 is greater than 20 K for clean and 10 K for the fouled tube. The tube 1 is situated in the region where the flue gas temperature is the highest. In the tube *a* the steam temperature increase is about 10 K for the clean tube surface while for the tube with outer ash deposits is only about 5 K. In this region, the flue gas temperature is of 196 K lower than the temperature of the flue gas at the inlet of the superheater. Therefore, increase in the steam temperature in the pipe *a* is smaller than in the pipe *l*.

SUPERHEATER WITH SCALE DEPOSITS ON THE INNER SURFACES OF THE TUBES

The calculations were conducted for the same superheater stage, i.e. for the first stage superheater. The tube inner surface is covered with a layer of scale deposits. In order to show the effect of internal scale deposits on the heat flow rate transferred from the flue gas to the steam, and the temperature of the superheater tubes, the following data for the first stage superheater have been adopted: $\delta_a = 0 \text{ m}$, $\delta_s = 0.0005 \text{ m}$, $k_s = 0.15 \text{ W/(m}\cdot\text{K)}$.

The heat transfer coefficient at the inner surface of the clean tube is $h_s = 2283.1 \text{ W/(m}^2\cdot\text{K)}$ while for the fouled tubes is larger and equal to $h_s = 2589.5 \text{ W/(m}^2\cdot\text{K)}$, since the steam velocity increases due to the smaller inner diameter of the tube with a layer of scales. The equivalent heat transfer coefficient defined by (Eq. 13) is $h_e = 264.2 \text{ W/(m}^2\cdot\text{K)}$. The results of the numerical simulation are shown in Fig. 8.

An inspection of the results depicted in figure 8 indicates that the internal scales have a large impact on the steam temperature. For the superheater with fouled tubes the steam temperature at the outlet of the superheater is about 25K lower compared to the superheater with clean tubes.

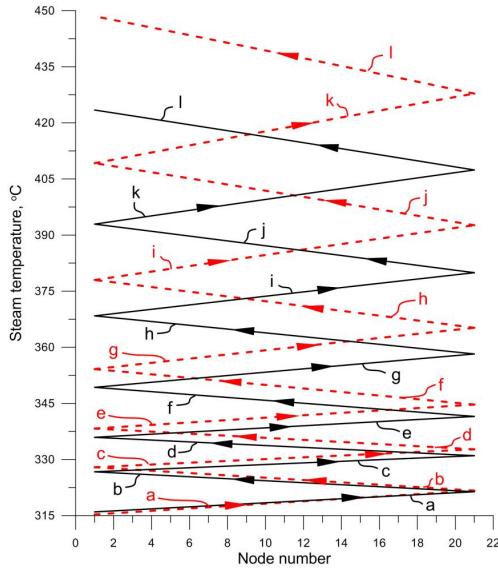


Fig. 8. Steam temperature changes along the steam flow path for clean (red dashed line) and fouled (black solid line) inner surfaces of the first stage superheater tubes.

Maximum tube wall temperature in superheater with scale deposits is $T_w = 528.2\text{ }^\circ\text{C}$ while for the superheater without scale deposits is $T_w = 465.2\text{ }^\circ\text{C}$ (Fig. 9). The heat flow rate transferred from the flue gas to the steam is equal to $\dot{Q}_c = 3.3394\text{ MW}$ for the clean superheater and the fouled superheater drops to $\dot{Q}_f = 2.8201\text{ MW}$. The relative decline in the superheater output defined as $100(\dot{Q}_c - \dot{Q}_f)/\dot{Q}_c$, is equal to 15.55%.

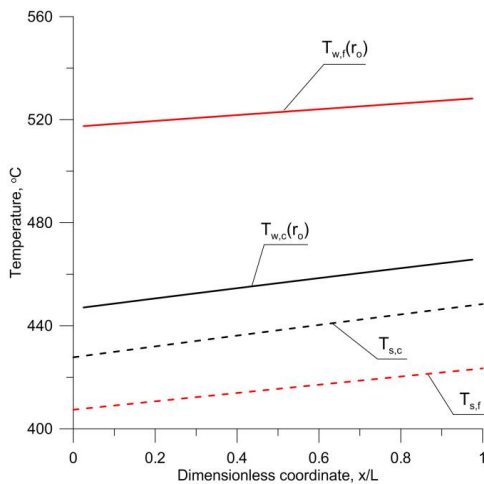


Fig. 9. Steam and tube wall temperature changes in the first stage superheater along the steam flow path in the tube l for the clean and fouled inner surfaces of the superheater tubes; $T_{s,c}$ and $T_{w,c}(r_o)$ - steam and tube wall temperature for clean tube, $T_{s,f}$ and

$T_{w,f}(r_o)$ - steam and tube wall temperature for tube with fouled inner surface.

This example shows the harmful effects of internal scale deposits on the operation conditions of the superheater. The heat flow rate decreases while increasing the maximum temperature of the metal, which in turn can lead to overheating of the tube material.

EXPERIMENTAL VERIFICATION

A computer system for monitoring of boiler slagging and fouling was installed in the power plant boiler OP-210M. The boiler is fired by pulverized hard coal. Test studies were performed with the installed system in real conditions to assess its effectiveness and accuracy. Mathematical models for each superheater stage have been developed to calculate the steam and flue gas temperature for each tube row. Also, the tube wall temperature along the steam flow path is determined.

The boiler simulation was carried out for the following data: the boiler steam output, $D = 49.47\text{ kg/s} = 178.1 \cdot 10^3\text{ kg/h}$, the lower calorific value of hard coal, $W_d = 21587\text{ kJ/kg}$, the excess air ratio, $\lambda = 1.16$. The resistance of ash deposits on the individual stages of superheaters was selected so that the steam temperatures calculated and measured at the outlet of each superheater stages are equal. The following values of thermal resistance $R = \delta_a / k_a$ were obtained:

- $R = 2.846 \cdot 10^{-2}\text{ m}^2\text{K/W}$ for platen superheater,
- $R = 2.425 \cdot 10^{-2}\text{ m}^2\text{K/W}$ for first stage superheater,
- $R = 4.375 \cdot 10^{-2}\text{ m}^2\text{K/W}$ for second stage superheater,
- $R = 4.375 \cdot 10^{-2}\text{ m}^2\text{K/W}$ for third stage superheater.

The average thermal efficiency of the combustion chamber walls determined from Eq. (12) is $\psi = 0.34$.

Comparison of calculated and measured steam temperature at the outlet of each stage and the temperature of the flue gas after every superheater stage is shown in Table 1.

The flue gas temperature at the outlet of the combustion chamber and before each superheater stage was calculated based on the flue gas temperature measured after the first superheater stage. Then the temperature of the flue gas before each superheater stage was determined sequentially, starting with the calculation of the flue gas temperature in front of the first stage. Based on the energy balance equation for the j -th superheater stage

$$\dot{m}_{s,j} \bar{c}_{ps,j} (T_{s,j}^{out} - T_{s,j}^{in}) = \dot{m}_{g,j} \bar{c}_{pg,j} (T_{g,j}^{in} - T_{g,j}^{out}) \quad (28)$$

Table 1. Comparison of calculated and measured steam temperature at the outlet of each stage and the temperature of the flue gas after every superheater stage

	Measured temperature, °C	Calculated temperature, °C
The temperature of saturated steam at the drum outlet	---	313.5
The steam temperature at outlet of the first stage superheater (before attemperator I)	392.0	391.5
The steam temperature at outlet of the first stage superheater (after attemperator I)	380.15	374.6
The steam temperature at outlet of the platen superheater (before attemperator II)	461.7	458.8
The steam temperature at outlet of the platen superheater (after attemperator II)	447.4	448.5
The steam temperature at outlet of the second stage superheater	---	492.0
The steam temperature at outlet of the third stage superheater	534.4	531.8
The flue gas temperature at outlet of the combustion chamber	1181.3	1208.7
The flue gas temperature after the platen superheater	1053,5	1040.4
The flue gas temperature after the convective evaporator I	1026.5	1018.7
The mean flue gas temperature after the second and third stage of the superheater	876,6	881.0
The flue gas temperature after the first superheater stage	690.5	693.5
The flue gas temperature after the convective evaporator II	663.5	664.9
The flue gas temperature at the outlet of the boiler	127.7	---

the flue gas temperature $T_{g,j}^{in}$ at the inlet of the j -th stage of the superheater can be obtained

$$T_{g,j}^{in} = \frac{\dot{m}_{s,j} \bar{c}_{ps,j}}{\dot{m}_{g,j} \bar{c}_{pg,j}} (T_{s,j}^{out} - T_{s,j}^{in}) + T_{g,j}^{out} \quad (29)$$

The steam temperature at the inlet $T_{s,j}^{in}$ and outlet of the superheater stage $T_{s,j}^{out}$, as well as the superheater flue gas temperature $T_{g,j}^{out}$ are known from measurements. The steam mass flow rate $\dot{m}_{s,j}$ was also measured, and the mass flow rate of the flue gas $\dot{m}_{g,j}$ was determined based on the known fuel mass flow rate \dot{m}_F .

The analysis of results presented in Table 1 indicates that the agreement of calculated and measured flue gas temperatures at the outlet of the combustion chamber and after various superheater stages is quite good.

CONCLUSIONS

Numerical modeling of steam boilers presented in the paper can be used for detailed analysis of flow and heat transfer in combustion chambers and superheaters.

Comparison of the results of calculations and measurements confirms the high accuracy of the mathematical model developed in the paper, which takes into account the processes of waterwalls slagging and ash fouling of superheater surfaces.

Numerical simulation of the superheater is an effective tool in the design, operation as well as in upgrading the superheaters.

Using mathematical models of the combustion chamber and the superheater stages, the deposition of slag and ash on the boiler heating surfaces can be assessed in on-line mode.

The average slagging degree for the waterwalls as well as the average fouling degrees for each superheater stage are determined in order to use selective cleaning with sootblowers.

When the limits of the slagging and fouling degrees are set, the sootblowers can be activated after exceeding the prescribed fouling degrees.

The presented method of modeling is a useful tool for analyzing the impact of the internal scales or outer ash fouling on the superheater operating conditions. Both ash deposits at the external and scales on the internal surfaces of the tubes contribute to the reduction of the steam temperature at the outlet of the superheater. Furthermore, scaling on the inner surface of the tubes results in a significant temperature rise and may lead to the tube damage. The proposed method of numerical modeling of the superheater can be used in the design of superheater and water heaters located in the convection pass of the boiler. It can also be useful in the study of mechanisms of ash fouling and scale build-up on the tube surfaces since the steam, flue gas and tube wall temperatures, which are important in the analysis of fouling processes, are known along the flow paths of the steam and flue gas. The calculation results of thermal superheater obtained by the

proposed method are in good agreement with the results of CFD modeling using ANSYS-CFX (Trojan, 2015).

NOMENCLATURE

\bar{c}_p	mean specific heat, J/(kg·K)
d_h	hydraulic diameter of the superheater tube (for a circular tube, this equals the inner diameter of the tube), m
f_1	steam inlet temperature, °C
f_2	flue gas inlet temperature, °C
h_e	equivalent heat transfer coefficient, W/(m ² ·K)
h_g	heat transfer coefficient on the flue gas side, W/(m ² ·K)
h_s	heat transfer coefficient at the inner tube surface, W/(m ² ·K)
k_a	ash deposit thermal conductivity, W/(m·K)
k_s	iron oxides or scales thermal conductivity, W/(m·K)
L_r	tube length, m
N	number of finite volumes on the tube length
M	parameter accounting for the kind of fuel (coal, oil or gas) and burners location
\dot{m}_b	mass flow rate of brine,
\dot{m}_F	fuel mass flow rate, kg/s
\dot{m}_s	steam mass flow rate per tube, kg/s
\dot{m}_g	flue gas mass flow rate per tube, kg/s
P	static pressure, Pa
\dot{Q}	heat flow rate, W
r	radius, m
r_a	outer radius of deposit layer, m
r_{in}	inner radius, m
r_o	outer radius, m
R	thermal resistance, m ² K/W
R_a	tube roughness, mm
s	coordinate along the flow path in direction of flow, m
s_1	longitudinal pitch perpendicular to the flue gas flow direction, m
s_2	longitudinal pitch parallel to the flue gas flow direction, m
T_{fe}	flue gas temperature at the furnace exit, °C
T_g	gas temperature, °C
\bar{T}_g	mean gas temperature over the row thickness, °C
T_{ge}	flue gas temperature after the superheater, °C

$T'_{g,i}$	gas temperature before the tube, °C
$T''_{g,i}$	gas temperature after the tube, °C
T_{gs}	flue gas temperature, °C
T_s	steam temperature, °C
$\bar{T}_{s,i}$	mean steam temperature, °C
T_w	tube wall temperature, °C
W_d	lower calorific value of coal, kJ/kg
w	steam velocity, m/s

Greek symbols

δ_a	thickness of ash deposits, m
δ_s	thickness of iron oxide or scale deposits, m
λ	excess air ratio
ε_f	emissivity of the combustion chamber
$\Delta\dot{m}_g$	mass flow rate of the flue gas through a control volume, kg/s
φ	angle between tube axis and horizontal plane
ρ	steam density, kg/m ³
ξ	friction factor
ζ	loss coefficient due to local pressure loss
ψ	waterwall effectiveness

Subscripts

a	ash
b	brine
c	clean
$calc$	calculated
cg	convection
e	effective or equivalent
F	fuel
f	furnace
g	gas
h	hydraulic
in	inner
$meas$	measured
o	outlet
out	outlet
rg	radiation
s	scale
w	wall

REFERENCES

- Hewitt, G.F., Shires G.L., Bott T.R. Process Heat Transfer. CRC Press - Begell House: Boca Raton; 1994.
- Wieland Ch., Kreutzkam B., Balan G., Spliethoff H. Evaluation, comparison and validation of deposition

criteria for numerical simulation of slagging. *Applied Energy* 2012; 93: pp. 184 – 92.

Weber R., Mancini M., Schaffel-Mancini N., Kupka T. On predicting the ash behavior using Computational Fluid Dynamics. *Fuel Processing Technology* 2013; 105: pp. 113 – 28.

Leppänen A., Tran H., Taipale R., Välimäki E., Oksanen A. Numerical modeling of fine particle and deposit formation in a recovery boiler. *Fuel* 2014; 129: pp. 45 – 53.

Blokh, A. G., Heat Transfer in Steam Boiler Furnace, Hemisphere Publishing Corporation, Washington, USA, 1988.

Kuznetsov, N. V., Mitor, V. V., Dubovskij, I. E., and Karasina, E. S., Standard Methods of Thermal Design for Power Boilers, (in Russian), Central Boiler and Turbine Institute, Energy, Moscow, Soviet Union, 1973.

Taler D., Taler J. Simplified analysis of radiation heat exchange in boiler superheaters. *Heat Transfer Engineering*, An International Journal, Volume 30, Issue 8, July 2009, pp. 661-669.

Manadilli G. Replace implicit equations with signomial functions. *Chemical Engineering* 1997; 104 (8): pp. 129-32.

Gaddis ES. Pressure Drop of Tube Bundles in Cross Flow. In: VDI Heat Atlas, Second Ed. Springer, Berlin-Heidelberg; 2010; L1.4: pp. 1076 – 91.

Trojan M. Computer modeling of a convective steam superheater. *Archives of Thermodynamics* 2015, Vol. 36, No. 1, pp. 125-137.